This is the author's version of a work that was accepted for publication in Atmospheric environment (Ed. Elsevier). Changes resulting from the publishing process, such as peer review, editing, corrections, structural formatting, and other quality control mechanisms may not be reflected in this document. Changes may have been made to this work since it was submitted for publication. A definitive version was subsequently published in Izquierdo, R., Àvila, A. and Alarcón, M. "Trajectory statistical of atmospheric transport patterns and trends in precipitation chemistry of a rural site in NE Spain in 1984-2009" in Atmospheric environment, vol. 61 (2012), p. 400-408.

DOI 10.1016/j.atmosenv.2012.07.060

Atmospheric transport patterns and trends in precipitation chemistry using trajectory statistical methods at a rural site in NE Spain, 1984-2009

Rebeca Izquierdo[1]*, Anna Avila[1] and Marta Alarcón[2]

(1) CREAF, Cerdanyola del Vallès 08193, Spain

(2) Departament de Física i Enginyeria Nuclear, Universitat Politècnica de Catalunya, c/ Urgell 187, 08036 Barcelona, Spain

*Corresponding author: rebeca@creaf.uab.cat Tel: +34935813420; Fax: +34935814151

Abstract

The aim of this study is to interpret the variation of precipitation chemistry during the last 25 years in Montseny (NE Spain) by taking into account the main air mass transport routes and emission sources. To this end, trajectory cluster analysis and source-receptor models were applied to an early monitoring period (1984-1993) and compared to a more recent one (1998-2009). A decrease of Atlantic advections and increase of African and European air flows was found. Cluster analysis and source-receptor approaches showed that this region is under the influence of natural and anthropogenic sources from the local and long-range scale. Sulphate and H^+ source areas extended over a vast stretch of central Europe in the early period, but were drastically reduced in the recent period, showing the effectiveness of pollution abatement measures for S. On the other hand, NO_3^- sources areas from central Europe strikingly increased. Ship emissions and industrialisation in Eastern Europe and North Africa seem to be acquiring a greater role in the recent period.

Key words: Mediterranean, long-range transport, precipitation, back-trajectories, cluster analysis, source-receptor model

1. Introduction

The atmospheric dynamics in the West Mediterranean Basin (WMB) is conditioned by complex interactions of climatic and topographic effects that include the Azores high-pressure system, continental thermal lows over the Iberian Peninsula (IP thereafter) and the Sahara, orographic effects of the coastal ranges surrounding the Mediterranean coast, marked seasonal variations in temperature, humidity and rainfall and the arrival of frequent African dust intrusions (Millán et al. 1997; Rodríguez et al. 2003). Linked to climate change, modifications in wind circulation and precipitation patterns have been predicted for the Mediterranean region (Giorgi and Lionello, 2008), as well as an increase of African air masses (Moulin et al. 1997).

A systematic investigation on the emission sources and the rainwater chemical composition is necessary to understand the consequences of pollution on ecosystems (Arsene et al. 2007). In Europe, the Convention on Long Range Transboundary Air Pollution (CLRTAP) launched several protocols to reduce sulphur and nitrogen emissions to the atmosphere in the 1970s. As a result, sulphur deposition steadily decreased throughout Europe in the last 30 years (Stoddard et al. 1999; Skjelkvale et al. 2005), but success has been more limited for nitrogen compounds (Gundersen et al. 2006).

Meteorological classification refers to the identification of distinct patterns that influence climate/weather-related variables (Riccio et al. 2007). Over the last several decades, Trajectory Statistical analysis Methods (TSMs) have been used to examine transport patterns and dynamical processes of air masses (Stohl, 1996, 1998). Cluster analysis has been widely used to categorize back trajectories (Dorling and Davies, 1995; Jorba et al. 2004) and to identify synoptic weather regimes and long-range transport patterns that affect air pollution (Cape et al. 2000; Salvador et al. 2007). Cluster analysis is used to classify the air mass origin arriving at a site, but it does not provide further information on the geographical location of potential source regions (Salvador et al. 2010). This is frequently resolved with TSMs which are helpful for estimating the spatial distribution of emissions based on measurements at a receptor site (Stohl, 1996; Begum et al. 2005). For the interpretation of source areas, the potential source contribution function (PSCF), Seibert's concentration field methodology (Seibert et al. 1994) and Stohl's redistributed model (Stohl, 1996) have been profusely used (Charron et al. 1998; Polissar et al. 2001; Hoh and Hites, 2004; Salvador et al. 2004).

The aim of this study is to characterize the synoptic climatology and long-range transport of air pollutants arriving in Montseny (NE Spain) in order to interpret the variation of precipitation chemistry during the last 25 years. To this end, we have used back-trajectories, cluster analysis and source-receptor models for an early monitoring period (1984-1993) which are compared to a more recent one (1998-2009).

2. Material and Methods

2.1. Study site

La Castanya station (LC, 41º46'N, 2º21'E, 700 m) is located in the Montseny mountains of the Pre-litoral Catalan Range. Long-term biogeochemical studies have been undertaken since the 1970s in a forest plot close to the atmospheric sampling site (Rodà et al. 1999). The site is amidst extensive holm-oak (*Quercus*

ilex L.) forests in the Montseny Natural Park, 40 km to the N-NE from Barcelona and 25 km from the Mediterranean coast (Fig.1). The climate in Montseny is meso-Mediterranean sub-humid, with high interannual precipitation variability (range: 503-1638 mm y^{-1}, mean: 840 mm y^{-1} at LC, from 1983-2009). Summer droughts are common and snow is sporadic. Mean air temperature was 9ºC during the period 1983-2000 at LC.

2.2. Sampling and chemical analysis

Precipitation was collected weekly at LC from August 1983 to July 2010 (no data from September 2000 to March 2002). Precipitation was collected with 2 open bulk-deposition collectors from January 1984-September 2000 and March 2007-July 2010, and with wet/dry collectors (ESM Andersen instruments, G78-1001) from April 2002-July 2004, February 2005-March 2007, and February 2009-July 2010. In the last period, bulk and wet-only deposition were sampled in parallel (only wet data reported here). Any detectable contamination (e.g. bird droppings) was annotated and the sample, discarded.

Samples were taken to CREAF where they were processed according to previously described protocols (Avila, 1996; Avila and Rodà, 2002). Conductivity, alkalinity and pH were measured in unfiltered samples within 48h of sampling. Samples were filtered through 0.45μm membrane filters and stored at -20ºC. Ion chromatography was used to determine the concentrations of Na^+, K^+, Mg^{2+}, Ca^{2+}, NH_4^+, Cl^-, NO_3^- and SO_4^{2-}. Data quality was evaluated by: (1) control solutions within analytical runs, and (2) an ionic ratio (cation sum/anion sum) by accepting a 20% variation about the central value (= 1.00).

Regression analysis was performed between wet-only and bulk-deposition data during the parallel sampling for each chemical compound and good correlations were obtained ($R>0.8$, $p<0.001$). Then, regressions between wet and bulk concentrations were used for each analyte to obtain a complete bulk-deposition database from 1984 to 2009. Years 2001, 2004 (for base cations) and 2005 were not included due to fragmentary sampling.

2.3. Cluster analysis

A daily meteorological analysis was undertaken based on 96-h isosigma back-trajectories at 12:00h UTC and 1500m asl by using the HYSPLIT (Hybrid Single-Particle Lagrangian Integrated Trajectory) 4.0 dispersion model from the Air Resources Laboratory (ARL, available at http://www.arl.noaa.gov/ready/hysplit4.html, Draxler and Rolph, 2003). This height can be taken as representative of the mean transport wind at a synoptic scale within the upper boundary layer. The meteorological input was obtained from the ARL (Air Resources Laboratory) reanalysis database for the early 10-year monitoring period (1984-1993), and from FNL (1998-2004) and GDAS (Global Data Assimilation System) (2005-2009) from the NCEP (National Center for Environmental Prediction) for the most recent period (1998-2009).

Cluster analysis statistically aggregate observations into clusters such that each of them is as homogeneous as possible with respect to the clustering variables (Sharma, 1996). To compose each

cluster, HYSPLIT has a grouping module based on variations in the Total Spatial Variance (TSV) between different clusters which is compared to the spatial variance (SPVAR) within each cluster component. The final number of clusters is determined by a change in TSV as clusters are iteratively paired (Draxler et al. 2009). This clustering methodology was applied to the daily trajectories obtained for an early (1984-1993) and recent (1998-2009) period at Montseny.

Our rain chemistry database consisted of weekly observations; however, trajectories were obtained daily. We estimated a daily chemical concentration for the days with precipitation by proportionally correcting weekly chemical concentrations by the precipitation contribution of the rainy days to the weekly amount. The rainy days within each week and their precipitation amount were obtained from records at LC, and from the AEMET stations (Spanish Meteorological Service) of Turó de l'Home and Tagamanent which are 7 and 8 Km distant from LC, respectively. Precipitation events of <3 mm were not included, and only the days with rainfall amount of >0.02 mm were considered for the determination of rain days within a week.

The interpretation of the back trajectories was complemented with meteorological synoptic maps and the DREAM dust forecast model (http://www.bsc.es/projects/earthscience/DREAM).

2.4. Source-receptor model

Source-receptor methodologies establish relationships between a receptor point and the probable source areas by associating each chemical concentration value with its corresponding back-trajectory. Daily 00:00h and 12:00h UTC 72-h back-trajectories at 1500 m asl were computed for rainy days in both study periods. A grid with 2601 cells of 1º x 1º latitude and longitude was superimposed on the integration trajectory field to map contributing areas.

Here, the Seibert methodology (Seibert et al. 1994), whereby a logarithmic mean chemical concentration is computed for each grid cell based on the residence time of the trajectories in the cells, was used:

$$\log C_{ij} = \frac{\sum_{l} n_{ijl} \log C_{l}}{\sum_{l} n_{ijl}}$$

where Cij is the concentration in the cell (i,j), l is the index of the trajectory, n_{ijl} is the number of time steps of the trajectory l in the cell (i,j), and C_l is the chemical concentration measured at the receptor point corresponding to the trajectory l. To reduce the cell's local variability (random noise), a smoothing was applied and the value of each cell was replaced by the average between the cell and its eight neighbouring cells. A final filter excluded cells with less than five end points, thus producing a more interpretable image. The obtained field map reflects each cell contribution to the chemical rain concentration at the receptor point.

Seibert's and PSCF methods were both computed and a sensitivity analysis to different factors was applied. Although the models were sensitive to all factors and they pointed to similar source areas, for simplicity only results from the Seibert's model will be here retained.

To quantitatively compare the obtained source-receptor maps with European emissions, NO_x and SO_2 EMEP emission inventory data were gridded at 1ºx1º cell resolution. Then, cell by cell Spearman's rank correlations were calculated between the emission data and model concentrations.

3. Results

3.1. General air flow transport patterns

Cluster analysis established 8 trajectory groups for both study periods (Fig 2; Table 1) which represented the general air flow pathways arriving at LC in terms of direction and wind speed at 1500m asl. Predominant transport regimes were similar in both study periods, and were classified as Northern flows (cluster 1), North-Western (cluster 2), Western (clusters 3, 4), South-Western (cluster 5), South-Eastern (cluster 6) and Regional recirculation (cluster 7). Exceptions were the fast-moving NW trajectories in 1984-1993 (cluster 8*a*) and north-eastern flows from central Europe in 1998-2009 (cluster 8*b*).

From Fig. 2 it can be seen that fast W flows contributed 7% in both periods, slow W flows decreased from 16% to 7%, whereas fast and moderate NW flows were roughly similar in the two study periods (16%-17%). The sum of Atlantic flows accounted for 39% and 31% of data in the early and recent period, respectively. North African transport increased slightly, due to the increase of SW flows (from 9% to 13%). European flows increased from 13% to 18%, this being related to a central Europe contribution (12% of data) which was absent in the earlier period. Regional recirculation contributed between 25-27% (Fig. 2).

Cluster occurrence by season is detailed in Table 1. The 8 back-trajectory clusters were grouped in four main geographic provenances: Atlantic (NW plus W air flows), European (N and NE), North African (SW and SE) and Regional-local. The Atlantic provenance dominated in all seasons (30-45%) except in summer when Regional circulations predominated (Table 1). The seasonal patterns for Atlantic and Regional provenances were similar for the two study periods but the Atlantic contribution decreased in the recent period. European flows increased in winter-spring (21-25%) and autumn (18%), and North African flows in spring-summer (22-35%, Table 1).

3.2. Air flow transport pathways for rainy days

Cluster analysis was applied to the subset of only rainy days, which produced 7 clusters (Fig. 3). Transport regimes for rainy days were: Northern (cluster 1), North-Western (clusters 2 and 3), Western (cluster 4), South-Western (cluster 5), South-Eastern (cluster 6) and Western Recirculation (WR, cluster 7), with a similar grouping for both study periods. Recirculation transport was the most frequent situation for rainy days, but it decreased from 27% to 21% between periods (Fig. 3). $Western_{fast}$ and south-eastern flows slightly decreased between periods (13 to 10% and 15 to 12%, respectively). Northern, $North\text{-}western_{fast}$ and South-western flows increased from 14 to 17%, 4 to 9% and 16 to 19%, respectively and $NW_{moderate}$ remained constant about 10% (Fig. 3).

Seasonal patterns for rain-day clusters are shown in Table 3, where grouping for broad geographical areas as in the previous section has been applied. In agreement with the precipitation seasonal regime in the

Mediterranean area rainy days were more frequent in spring and autumn, not changing between periods. Winter and spring precipitation originated predominantly from the Atlantic (30-36%), summer precipitation originated mostly from Europe (23-26%) and Regional recirculation (27-33%), and autumn precipitation was dominated by North African flows (38-49%).

3.3. Association of rain chemical composition with transport pathways

The rain chemical composition that characterised each cluster in the two periods is presented in Table 3. Precipitation (arithmetic mean) decreased from 14.8 mm in 1984-1993 to 10.0 mm in 1998-2009. Chemical concentrations were weighted by the precipitation amount (volume weighted means VWM, Table 3). The comparison of grand total VWMs for both study periods shows an increase of NO_3^- (22 to 31 μeqL^{-1}), NH_4^+ (23 to 29 μeqL^{-1}) and Ca^{2+} (60 to 65 μeqL^{-1}), and a decrease of SO_4^{2-} (47 to 33 μeqL^{-1}), H^+ (15 to 4.6 μeqL^{-1}) and Mg^{2+} (10 to 8.6 μeqL^{-1}) while Na^+ and Cl^- remained constant about 23 and 29 μeqL^{-1} respectively. In 1984-1993, northern and WR flows presented the highest H^+ (~20 μeqL^{-1}) while $NW_{moderate}$, the lowest (9.8 μeqL^{-1}). Notice that in the recent period cluster maximum H^+ concentrations (SE, 7.9 μeqL^{-1}) were lower than the lowest H^+ concentrations in the early period ($NW_{moderate}$, 9.7 μeqL^{-1}). Ammonium and nitrate showed maximum values in N-NW provenances for both periods. In the recent period concentrations from the SW were of similar magnitude. Sulphate also showed maximum concentrations for Northern flows and Regional recirculations in the early period, but both decreased steeply (from 63 to 36, and 52 to 30 μeqL^{-1} respectively) in the late period. Marine ions (Na^+, Cl^-, partly Mg^{2+}) presented high concentrations in southern and western flows, coming from the Mediterranean and Atlantic Ocean. Calcium, unexpectedly, presented high values in NW_{fast} (thus the Atlantic) in both periods. A closer look at those data showed that, in some occasions, NW clusters were influenced by African mineral dust even if air flows were coming from the North Atlantic. For example, for the rain episode from 31th October to 2nd November (total rain amount of 157mm) Ca^{2+} concentration was 176 μeqL^{-1}. Back-trajectories were from NW and W but also crossed over Morocco and the southern IP (Fig. 4a). The associated synoptic meteorology (Fig.4b) shows a low-pressure system over the IP and a high-pressure system over the eastern Mediterranean that triggers air masses from North Africa to south-eastern Spain and the Mediterranean, as also shown by the DREAM dust model (Fig. 4b). If Ca^{2+} mean concentrations are recalculated for NW flows excluding the episodes with an African influence (indicated as 'pure-Atlantic' in Table 3), their values are about halved and become closer to Ca^{2+} concentration reported at Montseny in pure Atlantic flows (Avila and Alarcón,1999).

3.4. Long term trends in chemical composition of precipitation and source receptor model results

Mann-Kendall time trend test of annual precipitation and ion VWM concentrations at LC from 1983 to 2009 showed significant decreasing trends for H^+ and SO_4^{2-} ($p<0.0001$) and an increasing trend for NO_3^- ($p<0.01$; Table 4), consistent with the comparison between periods outlined before. The rest of the analyzed ions did not show significant temporal trends.

A source receptor model was applied to ions with significant trends (SO_4^{2-}, H^+ and NO_3^-). This model indicated that SO_4^{2-} and H^+ in the initial period mostly originated in a broad area in central Europe (NE France, Benelux, west Germany and the North Sea; Fig. 5) although for H^+, an extension to western

Poland, Switzerland and northern Italy was identified. Spearman's correlations between SO_2 emissions and SO_4^{2-} model concentrations (as well as NO_x emissions and NO_3^- concentrations) indicate a close correspondence, as correlations were all significant at $p < 0.005$ (Table 5).

The reduction of SO_4^{2-} and H^+ concentrations in precipitation at LC for the last two decades was matched with a dramatic reduction of these European source areas (Fig. 5). Conversely, increasing NO_3^- concentrations in precipitation at Montseny were associated with an increase of source areas in central Europe which increased in extension and contribution to concentrations to the North Sea, northern France, eastern Germany, southern Poland, Austria and northern Italy (Fig. 5c).

Sulphate, in addition to its European origin, also presented an African source located in Western North Africa and central Algeria in the early period and only in central Algeria in the recent one (Fig. 5a). An African source area of NO_3^- only appeared in the recent period and was situated in central Algeria (Fig. 5c).

4. Discussion

4.1. Atmospheric regimes and seasonal patterns

Trajectories from the N, NW and W were more frequent in winter when the Azores high usually weakened and situated well to the west of its usual position (south of Azores), thus favouring the entry of Atlantic air masses to the Western Mediterranean. But in winter the Azores high can also stay for long periods close to the IP producing the stagnation of air masses over the Peninsula (Millán et al. 1997). This may account for the 17% occurrence of Regional recirculation in winter observed in this study.

In summer, the Azores high undergoes its highest intensity and is located to the east and north of its usual position, whereas thermal lows are developed over the IP and the Sahara (Millán et al. 1997). This accounts for the observed short trajectories with recirculation in the study region and for African fluxes. Our results matched similar trajectory cluster analysis for aerosol transport in the IP (Jorba et al. 2004; Borge et al. 2007; Salvador et al. 2008) and more specifically for aerosol data at LC (Pérez et al. 2008, Pey et al. 2009).

The seasonal analysis for rainy days indicated that precipitation in winter and spring originated mostly from the Atlantic, in autumn from North Africa and in summer, from Europe and the Regional recirculation (Table 2). This was similar to previous classifications at LC based on meteorological synoptic maps and trajectory analysis (Avila and Alarcón, 1999).

4.2. Decadal trends, air mass transport and potential source areas of precipitation chemical compounds

Spearman's correlation coefficients between modelled concentrations and EMEP emission data were highly significant (Table 5), supporting the validity of the source-receptor model to indicate pollutant

contributing areas. Concentration maps from the source-receptor model in the period 1984-1993 pointed to north-eastern France, Benelux, Germany and the North Sea (Fig.5a) as source areas for SO_4^{2} and NO_3^- and acidity. A similar geographic source area for these components was obtained with PSCF, Seibert's and Stohl's (1996) methodologies at a site in central France considering the period 1992-1995 (Charron et al. 1998) which can be compared with our early period. In the recent period, a drastic reduction of the transported acidity was observed, which indicates that sulphate was the main contributor to acidity. For acidity source areas shifted and main contributing areas are now located in eastern Europe.

The simultaneous decline of SO_4^{2-} and H^+ rain concentrations observed from 1983 to 2009 at LC (Table 3) can be related with localised SO_2 emission decrease (SO_4^{2-} in regional fluxes decreasing from 52 to 30 μeqL^{-1}) and to general declines throughout Europe as indicated by a SO_4^{2-} decrease from 63 to 36 μeqL^{-1} in the N cluster (Table 3). The reduction of high concentration source areas in central Europe (Fig. 5a) confirms this observation. On the other hand, the observed increasing NO_3^- trend is consistent with that observed at other sites in Catalonia (Avila et al. 2010). Cluster classification in this study showed that NO_3^- increased in all clusters, but the increase was more prominent for NW and SW fluxes, roughly doubling in the recent period (Table 3). Nitrate sources in Europe were extended over larger areas and their contribution to concentrations was intensified (Fig. 5c).

European S (and sometimes N) emissions on land are being successfully abated; however, recent studies indicate the increasing role of maritime emissions (Endresen et al. 2003; Collins et al. 2008). The commercial shipping contribution has been estimated at 5-8% of global anthropogenic SO_2 emissions and 15-30% of global fossil fuel NO_x emissions (Eyring et al. 2005). In the North Sea, intense ship traffic to Rotterdam and Hamburg is responsible for an increase in SO_4^{2-}, NO_3^- and NH_4^+ aerosol concentrations by 50% in summer around this area (Matthias et al. 2010). The implementation of a sulphur emission control area (SECA) in the North Sea in 2007 was found to reduce SO_2 and SO_4^{2-} aerosol concentrations, though NO_3^- concentrations slightly increased (Matthias et al. 2010). In our study, the high SO_4^{2-} and NO_3^- concentrations from N and $NW_{moderate}$ clusters and the modelled source area over the North Sea (Fig. 5a,c) may be related with these increasing maritime pollutant emissions.

On the other hand, large recent SO_2 emission reductions in Europe have played an important role in modifying nitrate aerosol concentrations. Since atmospheric ammonia is first used to neutralize sulphate to form ammonium sulphate aerosols, particulate nitrate can only be formed if excess ammonia is available. With declining SO_2 in the atmosphere, nitrate aerosol concentrations have been found to be 25% higher than expected if SO_2 emissions were not reduced. This effect has been especially large in Central and East Europe (Fagerli and Aas, 2008) and may have contributed to the increase of NO_3^- rain concentration at LC observed in N and NW clusters. Ammonium aerosols resulting from NH_3 combination with sulphuric and nitric acids can be transported over several thousand kilometres (Hov and Hjollo, 1994; Charron et al 1998). Ammonium nitrate aerosols are thermically unstable at >20ºC and this might not be properly represented in current source-receptor methodologies, such as the Seibert's method here used. To our knowledge trajectory models have not yet incorporated modules considering chemical transformations during transport, nor wet deposition processes.

Trajectories from North Africa are highly enriched in NO_3^- in the recent period and their SO_4^{2-} concentrations were similar to those of northern air fluxes (Table 3). Furthermore, source receptor maps showed high SO_4^{2-} in southern Morocco and Central Algeria (Fig.5a). Recent studies of African aerosols have shown that SO_4^{2-} in dust particles can be attributed to the dissolution of dolomite (CaMgCO3) and calcium sulphate derived from gypsum soils and salt-lakes in specific areas of North Africa (Rodríguez et al. 2011), but these authors provide also detailed evidence of the influence of industrial activities being developed in North Africa (involving crude oil refineries, phosphate fertilizer industry, and power plants) that have an influence on NO_3^-, NH_4^+ and at least 60% of SO_4^{2-} of <10 μm content in particles transported in the Saharan Air Layer (Rodríguez et al., 2011).

Conclusions

Back-trajectory clustering showed a decrease of Atlantic advections and an increase of African and European air flows. Precipitation in winter and spring predominantly originated from the Atlantic, in autumn from North Africa, and in summer, European and Regional recirculation flows contributed similarly.

A significant decrease of SO_4^{2-} and H^+ and an increase of NO_3^- was found in bulk deposition in Montseny. Cluster analysis and a source-receptor model indicated that NE Spain is under the influence of natural and anthropogenic sources from the local scale and long-range transport. The reduction of SO_4^{2-} and H^+ concentrations in precipitation at LC for the last two decades was matched with a dramatic reduction of source areas in central Europe. For NO_3^-, initial small source areas in central Europe expanded towards the North Sea, northern France, eastern Germany, southern Poland, Austria and northern Italy. Ship emissions and the growing industrialisation in Eastern Europe and North Africa probably explains the location of the pollutants' main source areas in the recent period.

Acknowledgements We acknowledge the financial support from the Spanish Government (CGL2009-13188-C03-01, CGL2009-11205, CSD2008-00040-Consolider Montes grants and CSD 2007-00067-Consolider GRACCIE). Mirna Lopez is thanked for assistance with back-trajectory analysis.

310 References

311 Arsene, C., Olariu, R.I. and Mihalopoulos, N. 2007. Chemical composition of rainwater in the northeastern
312 Romania, Iasi region (2003-2006). Atmospheric Environment 41, 9452-9467.

313 Avila, A. 1996. Time trends in the precipitation chemistry at a mountain site in Northeastern Spain for the
314 period 1983-1994. Atmospheric Environment 30, 1363-1373.

315 Avila, A., Alarcón, M. 1999. Relationship between precipitation chemistry and meteorological situations at a
316 rural site in NE Spain. Atmospheric Environment 33, 1663-1677.

317 Avila, A., Rodà, F. 2002. Assessing decadal changes in rainwater alkalinity at a rural Mediterranean site in
318 the Montseny Mountains (NE Spain). Atmospheric Environment 36, 2881-2890.

319 Avila, A., Molowny-Horas, R., Gimeno, B.S., Peñuelas, J. 2010. Analysis of decadal time series in wet N
320 concentrations at five rural sites in NE Spain, Water Air & Soil Pollution 207 (1-4), 123-138, doi.
321 10.1007/s11270-009-0124-7

322 Begum, B.A., Kim, E., Jeong, C., Lee, D., Hopke. P.K. 2005. Evaluation of the potential source contribution
323 function using the 2002 Quebec forest fire episode. Atmospheric Environment 39, 3719-3724.

324 Borge, R., Lumbreras, J., Vardoulakis, S., Kassomenos, P., Rodríguez, E. 2007. Analysis of long-range
325 transport influences on urban PM_{10} using two-stage atmospheric trajectory clusters. Atmospheric
326 Environment 41, 4434-4450.

327 Cape, J.N., Methven, J., Hudson, L.E. 2000. The use of trajectory cluster analysis to interpret trace gas
328 measurements at Mace Head, Ireland. Atmospheric Environment 34, 3651-3663.

329 Charron, A., Plaisance, H., Sauvage, S., Coddeville, P., Galloo, J.C., Guillermo, R. 1998. Intercomparison
330 between three receptor-oriented models applied to acidic species in precipitation. The Science of the Total
331 Environment 223, 53-63.

332 Charron, A., Plaisance, H., Sauvage, S., Coddeville, P., Galloo, J.C., Guillermo, R. 2000. A study of the
333 source-receptor relationships influencing the acidity of precipitation collected at a rural site in France.
334 Atmospheric Environment 34, 3665-3674.

335 Collins, W., Sanderson, M.G., Johnson, C. 2008. Impact of increasing ship emissions on air quality and
336 deposition over Europe by 2030. Meteorologische Zeitschrift 18, 25-39.

337 Dorling, S.R., Davies, T.D. 1995. Extending cluster analysis – synoptic meteorology links to characterise
338 chemical climates at six north-west European monitoring stations. Atmospheric Environment 29(2), 145-
339 167.

340 Draxler, R.R., Rolph, G.D. 2003. HYSPLIT (HYbrid Single-Particle Lagrangian Integrated Trajectory) Model
341 access via NOAA ARL READY website (http://www.arl.noaa.gov/ready/hysplit4.html). NOAA Air Resources
342 Laboratory, Silver Spring, MD.

343 Draxler, R.R., Stunder, B., Rolph, G., & Taylor, A. 2009. HYSPLIT_4 User's Guide. NOAA Air Resources
344 Laboratory (http://www.arl.noaa.gov/documents/reports/hysplit_user_guide.pdf,).

345 Endresen, Ø., Sørgård, E., Sundet, J.K., Dalsøren, S.B., Isaksen, I.S.A., Berglen, T.F., Gravir, G. 2003.
346 Emissions from international sea transportation and environmental impact. Journal of Geophisical
347 Research 108 (D17), 4560. Doi :10.1029/2002JD002898.

348 EMEP, 2011. Transboundary acidification, eutrophication and ground level ozone in Europe in 2009. EMEP
349 Status Report 1/11. Joint MSC-W & CCC & CEIP Report. Available from: www.emep.int

350 Eyring, V., Köhler, H.W., van Aardenne, J., Lauer, A. 2005. Emissions from international shipping: 1. The
351 last 50 years. Journal of Geophysical Research-Atmospheres 110 (D17), D17305.

352 Fagerli, H., Aas, W. 2008. Trends of nitrogen in air and precipitation: Model results and observation at
353 EMEP sites in Europe, 1980-2003. Environmental Pollution, 448-461.

354 Giorgi, F, Lionello, P. 2008. Climate change projections for the Mediterranean region. Global and Planetary
355 Change 63, 90-104. Doi:10.1016/j.gloplacha.2007.09.005

356 Gundersen, P., Schmidt, I.K., Raulund-Rasmussen, K. 2006. Leaching of nitrate from temperate forests -
357 Effects of air pollution and forest management. Environmental Reviews 14 (1), 1-57. Doi: 10.1139/a05-015.

358 Hoh, E. and Hites, R.A. 2004. Sources of toxaphene and other organochlorine pesticides in North America
359 as determined by air measurements and potential source contribution function analyses. Environmental
360 Science & Technology 38, 4187-4194.

361 Hov, O., Hjollo, B.A. 1994. Transport distance of ammonia and ammonium in Northern Europe. 2. Its
362 relation to emissions of SO_2 and NO_x. Journal of Geophysical Research 99, 18749-18755.

363 Jorba, O., Pérez, C., Rocadensbosch, F., Baldasano, J.M. 2004. Cluster analysis of 4-day back trajectories
364 arriving in the Barcelona area, Spain, from 1997 to 2002. Journal of Applied Meteorology 43, 887-901.

365 Matthias, V., Bewersdorff, I., Aulinger, A., Quante, M. 2010. The contribution of ship emissions to air
366 pollution in the North Sea regions. Environmental Pollution 158, 2241-2250.

367 Millán M., Salvador R., Mantilla E., Kallos G. 1997. Photo-oxidant dynamics in the Mediterranean basin in
368 summer: results from European research projects. Journal of Geophysical Research 102, 8811-8823.

369 Moulin, C., Lambert, C.E., Dulac, F., Dayan, U. 1997. Control of atmospheric export of dust from North
370 Africa by the North Atlantic Oscillation. Nature 387, 691-694.

371 Pakkanen, T.A. 1996. Study of formation of coarse particle nitrate aerosol. Atmospheric Environment 30,
372 2475-2482.

373 Pérez, N., Pey, J., Castillo, S., Viana, M.M., Alastuey, A., Querol, X. 2008. Interpretation of the variability of
374 levels of regional background aerosols in the Western Mediterranean. Science of the Total Environment
375 407, 527-540.

376 Pey, J., Pérez, N., Castillo, S., Viana, M., Moreno, T., Pandolfi, M., López-Sebastián, J.M., Alastuey, A.,
377 Querol, X. 2009. Geochemistry of regional background aerosols in the Western Mediterranean.
378 Atmospheric Research 94, 422-435.

379 Polissar, A.V., Hopke, P.K., Harris, J.M. 2001. Source regions for atmospheric aerosol measured at Barrow,
380 Alaska. Environmental Science & Technology 35, 4214-4226.

381 Querol, X., Alastuey, A., Puigcercus, J.A., Mantilla, E., Miró, J.V., López-Soler, A., Plana, F. and Artiñano,
382 B. 1998 Seasonal evolution of suspended particles around a large coal-fired power station: Particle levels
383 and sources. Atmospheric Environment 32, 1963-1978.

384 Riccio, A., Giunta, G., Chianese, E. 2007. The application of a trajectory classification procedure to
385 interpret air pollution measurements in the urban area of Naples (Southern Italy). Science of the Total
386 Environment 376, 198-214.

387 Rodà, F., Retana, J., Gracia, C.A., Bellot, J. 1999 Ecology of Mediterranean Evergreen Oak Forests.
388 Ecological Studies 137 (373pp). Springer. Berlin.

389 Rodríguez, S., Alastuey, A., Alonso-Pérez, S., Querol, X. Cuevas, E., Abreu-Afonso, J., Viana, M., Pandolfi,
390 M., de la Rosa, J. 2011. Transport of desert dust mixed with North African industrial pollutants in the
391 subtropical Saharan Air Layer. Atmospheric Chemistry and Physics Discussions 11, 8841-8892. Doi:
392 10.5194/acpd-11-8841-2011.

393 Rodríguez, S., Querol, X., Alastuey, A., Mantilla, E. 2003. Events affecting levels and seasonal evolution of
394 airborne particulate matter concentrations in the Western Mediterranean. Environmental Science and
395 Technology 37, 216-222.

396 Salvador, P., Artiñano, B., Alonso, D.G., Querol, X., Alastuey, A. 2004. Identification and characterisation of
397 sources of PM_{10} in Madrid (Spain) by statistical methods. Atmospheric Environment 38, 435-447.

398 Salvador, P., Artíñaño, B., Querol, X., Alastuey, A., Costoya, M. 2007. Characterisation of local and
399 external contributions of atmospheric particulate matter at a background coastal site. Atmospheric
400 Environment 41, 838-845.

401 Salvador, P., Artíñano, B., Querol, X., Alastuey, A. 2008. A combined analysis of backward trajectories and
402 aerosol chemistry to characterise long-range transport episodes of particulate matter: The Madrid air basin,
403 a case of study. Science of Total Environment 390, 495-506. Doi: 10.1016/j.scitotenv.2007.10.052.

Salvador, P., Artíñano, B., Pio, C., Afonso, J., Legrand, M., Puxbaum, H., Hammer, S. 2010. Evaluation of aerosol sources at European high altitude background sites with trajectory statistical methods. Atmospheric Environment 44, 2316-2329.

Seibert P., Kromp-Kolb H., Balterpensger U., Jost D.T., Schwikowski M., Kasper A., Puxbaum H. 1994. Trajectory analysis of aerosol measurements at high alpine sites. In: P.M. P. Borrell, T. Cvitas and W. Seiler (Eds.) Transport and Transformation of Pollutants in the Troposphere. Academic Publishing, Den Haag. pp 689-693.

Sharma, S. 1996. Applied Multivariate Techniques. John Wiley & Sons, Inc. New York, pp.493

Skjelkvale, B.L. and 14 authors. 2005. Regional scale evidence for improvements in surface water chemistry 1990-2001. Environmental Pollution 137, 165-176.

Stoddard, J.L. and 22 authors. 1999. Regional trends in aquatic recovery from acidification in North America and Europe. Nature 401, 575-578

Stohl, A. 1996. Trajectory statistics – A new method to establish source-receptor relationships of air pollutants and its applications to the transport of particulate sulphate in Europe. Atmospheric Environment 30, 579-587.

Stohl, A. 1998. Computation, accuracy and applications of trajectories - a review and bibliography. Atmospheric Environment 32, 947-966.

Tables

Table 1. Seasonality of atmospheric transport regimes for early 10-years monitoring period (1984-1993) and the more recent one (1998-2009): frequency of back-trajectories associated to each cluster and frequency of clusters associated to each provenance (%). Winter: December-February, spring: March-May, summer: June-August and autumn: September-November.

Period 1984-1993						Period 1998-2009					
Cluster classification	N	Winter	Spring	Summer	Autumn	Cluster classification	N	Winter	Spring	Summer	Autumn
C1. N	492	16.5	16.0	10.7	10.8	C1. N	275	9.0	7.3	2.1	6.9
C2. NW_{fast}	303	12.5	8.8	4.7	7.3	C2. NW_{fast}	742	20.8	16.7	12.4	18.2
C3. W_{fast}	240	12.5	5.3	2.2	6.4	C3. W_{fast}	313	12.4	8.8	2.1	5.4
C4. W_{slow}	602	15.5	16.1	17.5	16.8	C4. W_{slow}	307	7.7	8.4	5.4	6.7
C5. SW	344	7.2	6.8	11.6	12.0	C5. SW	569	7.7	11.3	18.9	14.2
C6. SE	421	14.2	11.6	6.5	13.8	C6. SE	521	9.7	10.5	15.8	11.8
C7. Regional recirculation	985	17.1	26.1	38.6	25.9	C7. Regional recirculation	1106	17.2	23.1	35.4	25.6
C8*a*. $NW_{moderate}$	266	4.5	9.2	8.3	7.0	C8*b*. NE	532	15.5	14.0	8.0	11.3
Provenances						Provenances					
Atlantic (NW+W)	1411	45.1	39.5	32.6	37.5	Atlantic (NW+W)	1362	40.9	33.9	19.8	30.3
Europe (N)	492	16.5	16.0	10.7	10.8	Europe (N+NE)	807	24.5	21.3	10.1	18.2
North Africa (SW+SE)	765	21.4	18.5	18.2	25.8	North Africa (SW+SE)	1090	17.4	21.7	34.7	25.9
Regional - Local	985	17.1	26.1	38.6	25.9	Regional - Local	1106	17.2	23.1	35.4	25.6

Table 2. Seasonality of atmospheric transport regimes for rainy days in both study periods: frequency of back-trajectories associated to each cluster and frequency of clusters associated to each provenance (%). Winter: December-February, spring: March-May, summer: June-August and autumn: September-November.

Period 1984-1993						Period 1998-2009					
Cluster classification	N	Winter	Spring	Summer	Autumn	Cluster classification	N	Winter	Spring	Summer	Autumn
C1. N	101	9.8	22.5	25.9	11.4	C1. N	108	17.4	18.1	22.9	13.5
C2. $NW_{moderate}$	46	2.9	10.0	11.1	7.0	C2. $NW_{moderate}$	66	8.3	12.6	13.8	8.4
C3.NW_{fast}	25	6.9	6.0	2.8	1.9	C3.NW_{fast}	50	14.4	10.7	0.9	4.5
C4. W_{fast}	78	20.6	13.5	11.1	11.4	C4. W_{fast}	61	12.9	7.9	8.3	11.6
C5. SW	100	14.7	14.5	11.1	27.8	C5. SW	109	10.6	14.9	22.0	25.2
C6. SE	75	21.6	7.5	4.6	20.9	C6. SE	73	18.2	10.7	5.5	12.9
C7. WR	143	23.5	26.0	33.3	19.6	C7. WR	144	18.2	25.1	26.6	23.9
Provenances						Provenances					
Atlantic (NW+W)	149	30.4	29.5	25.0	20.3	Atlantic (NW+W)	177	35.6	31.2	22.9	24.5
Europe (N)	101	9.8	22.5	25.9	11.4	Europe (N+NE)	108	17.4	18.1	22.9	13.5
North Africa (SW+SE)	175	36.3	22.0	15.7	48.7	North Africa (SW+SE)	182	28.8	25.6	27.5	38.1
Regional - Local	143	23.5	26.0	33.3	19.6	Regional - Local	144	18.2	25.1	26.6	23.9
TOTAL	568	18.0	35.2	19.0	27.8	TOTAL	611	21.6	35.2	17.8	25.4

Table 3. Rain volume (arithmetic mean, mm) and volume-weighted mean (VWM) concentrations (in μeqL^{-1}) for the analysed chemical species and for each cluster in both study periods

1984-1993 period	Rain	N cations	N anions	H^+	Na^+	Ca^{2+}	Mg^{2+}	NH_4^+	NO_3^-	SO_4^{2-}	Cl^-
C1. N	8.9	101	101	20.0	15.4	60.0	10.1	37.8	32.0	63.5	20.8
C2. $NW_{moderate}$	10.9	46	46	9.7	19.1	46.8	8.5	23.5	21.5	41.6	23.9
C3*a*.NW_{fast}	9.0	25	25	13.1	21.5	80.7	11.3	30.7	23.3	53.5	25.9
C3*b.* NW_{fast} *modified*	9.4	22	22	13.5	19.4	49.7	9.6	32.3	22.9	47.8	23.4
C4. W_{fast}	12.9	78	78	14.9	18.8	49.5	9.2	24.5	20.5	45.9	24.4
C5. SW	16.9	100	100	11.0	29.3	87.3	11.8	18.6	20.8	46.6	36.1
C6. SE	26.2	75	75	12.2	27.4	58.5	10.1	14.7	15.1	36.6	34.3
C7. WR	14.9	143	143	20.4	20.2	46.2	9.9	27.0	25.5	51.8	26.0
Total	14.8	568	568	15.1	23.0	60.2	10.2	23.2	21.9	47.2	29.1
1998-2009 period											
C1. N	5.9	89	108	2.6	14.3	52.7	6.8	38.5	35.2	36.4	18.4
C2*a*. $NW_{moderate}$	5.6	55	66	2.4	46.1	119	16.0	34.4	44.2	46.9	54.2
C2*b*. $NW_{moderate}$ *modified*	4.4	43	54	3.7	21.6	55.2	8.7	41.3	42.3	37.5	25.1
C3. NW_{fast}	7.1	45	50	5.6	31.3	60.8	10.4	26.0	26.9	30.4	36.0
C4. W_{fast}	9.3	56	61	5.3	28.8	52.8	10.1	21.3	22.2	26.8	35.3
C5. SW	12.9	94	109	3.2	19.0	79.9	8.1	31.2	40.6	37.4	27.5
C6. SE	13.9	72	73	7.9	24.1	53.8	7.1	27.1	20.7	28.6	23.6
C7. WR	12.1	134	144	4.7	19.8	60.6	7.9	27.0	29.1	30.4	25.7
Total	10.0	545	611	4.6	22.9	65.9	8.6	29.0	31.1	33.0	28.3

Table 4. Mann-Kendall trend tests applied to annual volume-weighted mean concentrations (in μeq L^{-1}) in bulk deposition and to precipitation amount (in L m^{-2}) from 1983 to 2009 at LC, Montseny (no data from 2001, 2004 and 2005).

	N	Kendall Tau	p
Precipitation	24	-0.87	0.55
H^+	24	-0.61	0.00003
Na^+	24	0.17	0.25
Ca^{2+}	24	-0.07	0.62
Mg^{2+}	24	0.14	0.92
NH_4^+	24	-0.02	0.88
NO_3^-	24	0.38	0.0099
SO_4^{2-}	24	-0.58	0.00007
Cl^-	24	0.04	0.77

Table 5. Spearman's rank correlation coefficients (R) for concentrations vs. EMEP emission values. Early period = 1983-1994; recent period = 1998-2009.

	Valid N	R	p
NOx- NO_3^- early period	976	0.38	<0.000001
NOx – NO_3^- recent period	1042	0.17	<0.000001
SO2- SO_4^{2-} early period	976	0.26	<0.000001
SO2- SO_4^{2-} recent period	1042	0.09	0.004

Figures

Figure 1. Map of La Castanya study site (LC). NE Spain.

Figure 2. Cluster centroids and frequency of back-trajectories associated to each cluster for both study periods. Back-rajectories (72h) from the LC site, calculated at 1500m asl.

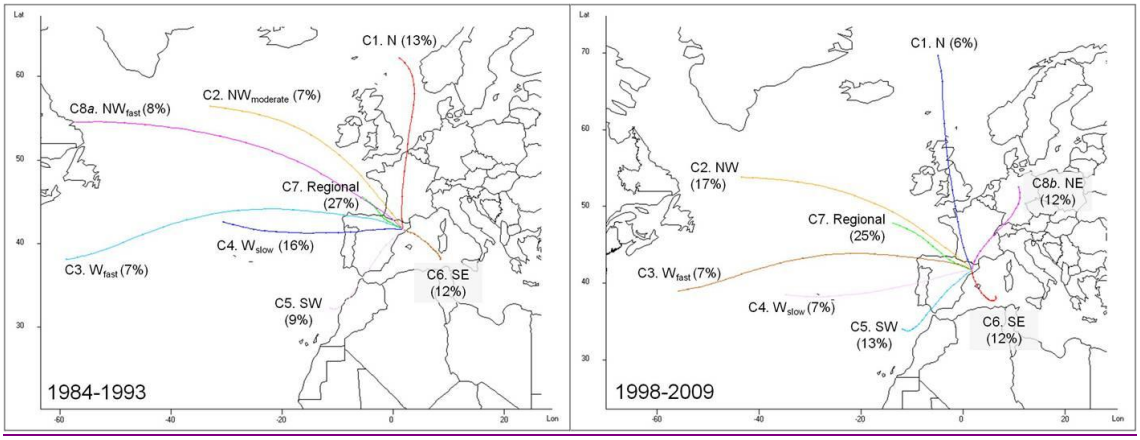

Figure 3. Cluster centroids and frequency of back-trajectories associated to each cluster for rainy days in both study periods at the LC site. Back-rajectories (72h) calculated at 1500m asl.

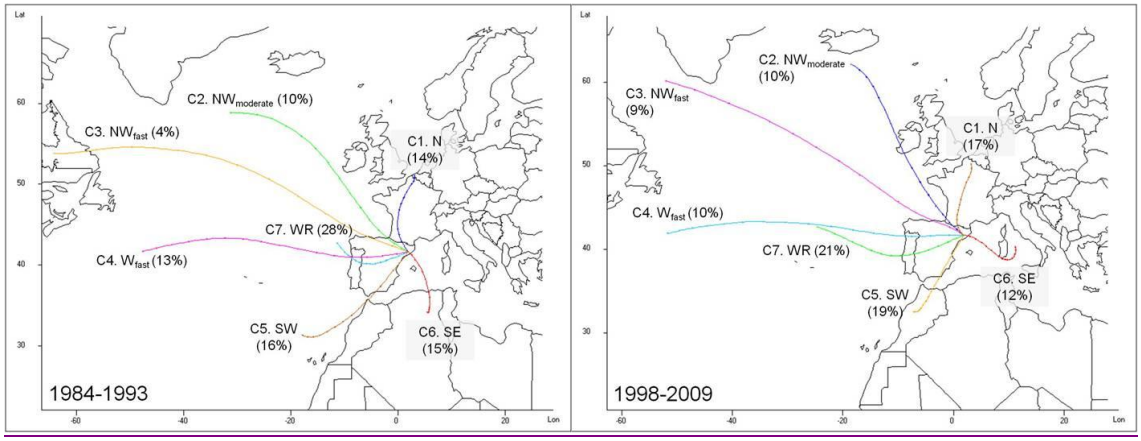

Figure 4. Study case of combined transport for rain days form 31 October 2008 to 2 November 2008: a) back-trajectories of rainy days and its cluster classification; b) synoptic and DREAM dust model maps for rainy days.

a)

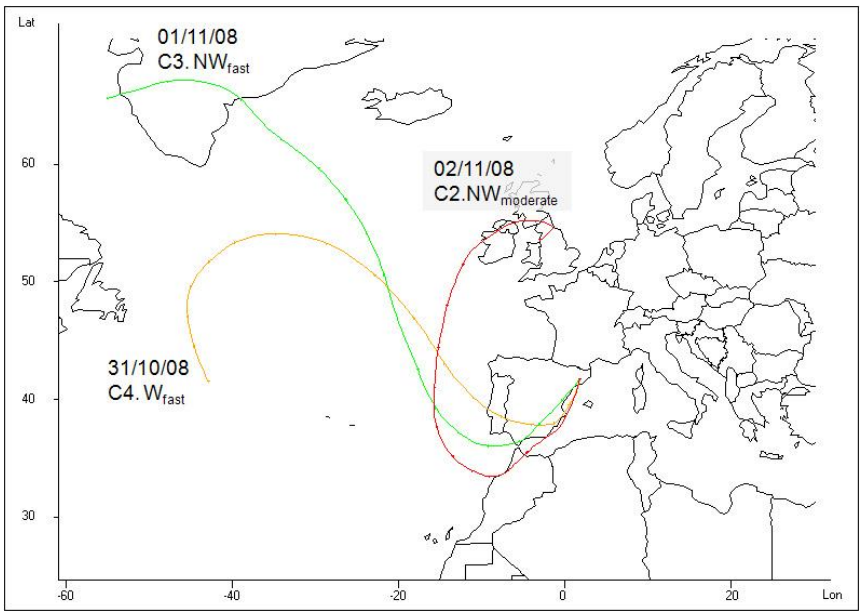

b)

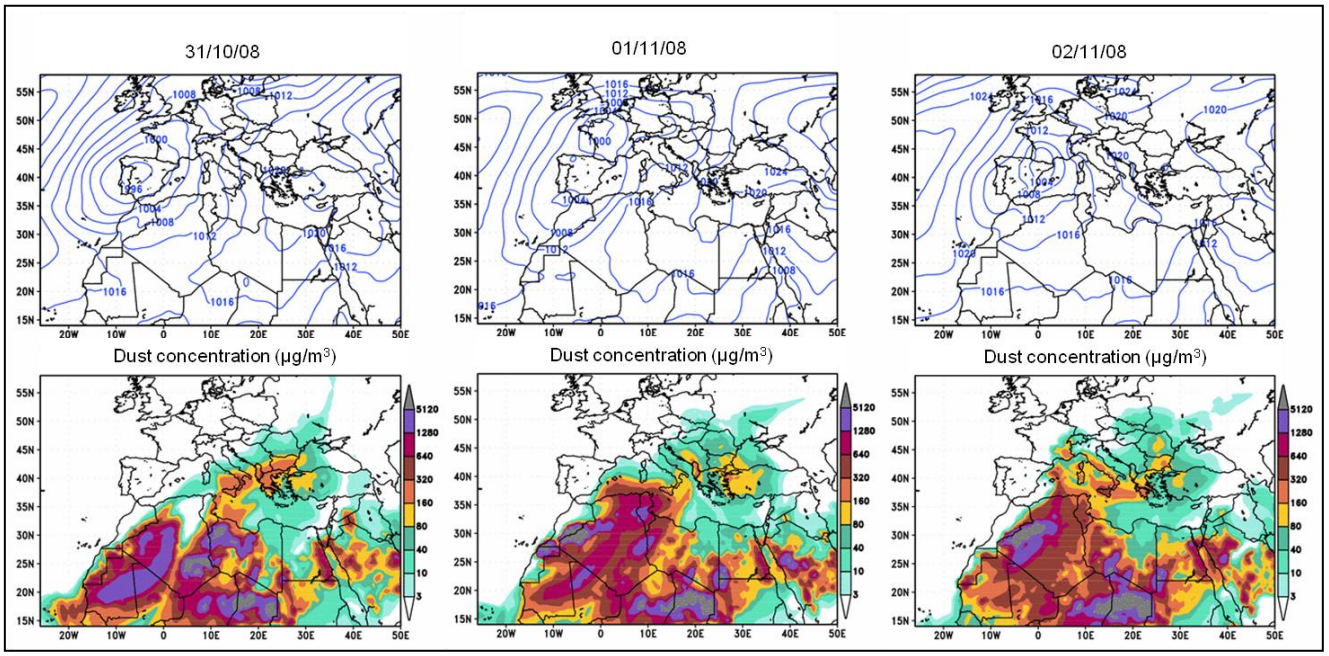

Figure 5. Source receptor concentrations maps (μeqL^{-1})

a) Sulphate (SO_4^{2-})

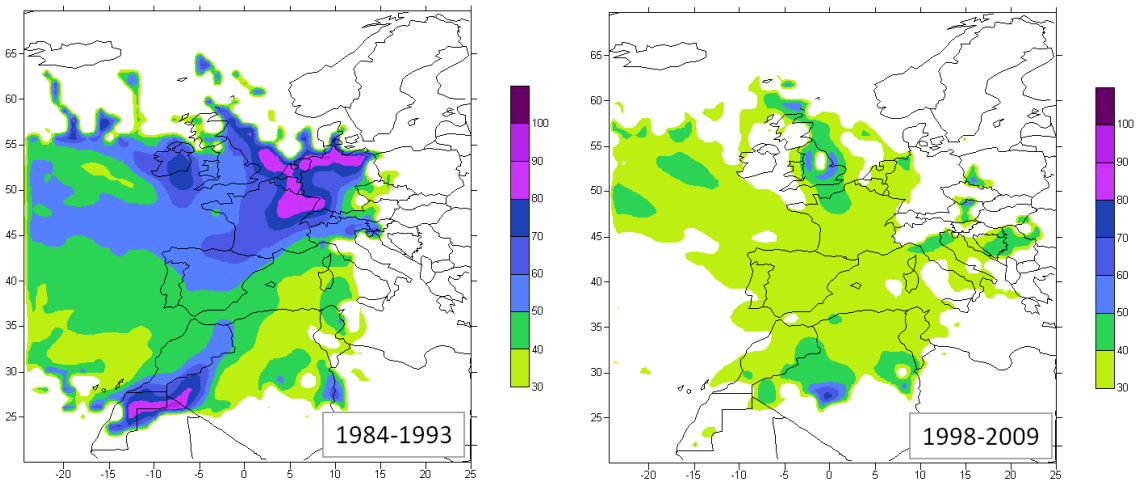

b) Hydrogen ion (H^+)

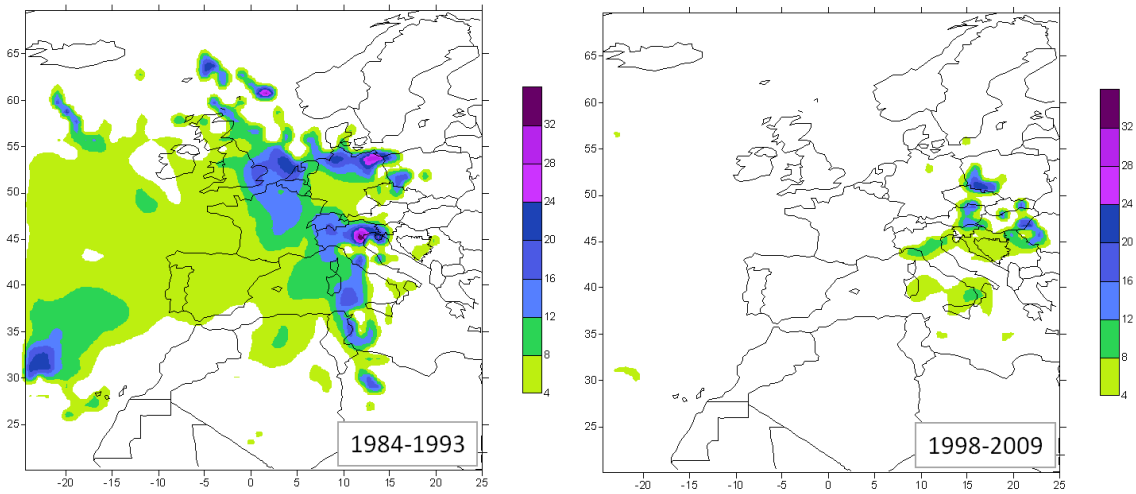

c) Nitrate (NO_3^-)